Magnetic domain characterizations of anisotropic-shaped MnAs nanoclusters position-controlled by selective-area metal-organic vapor phase epitaxy

Shingo Ito,[1] Shinjiroh Hara,[1,2,a)] Toshitomo Wakatsuki,[1] and Takashi Fukui[1]
[1]*Research Center for Integrated Quantum Electronics and Graduate School of Information Science and Technology, Hokkaido University, North 13 West 8, Sapporo 060-8628, Japan*
[2]*PRESTO, Japan Science and Technology Agency, 4-1-8 Honcho, Kawaguchi 332-0012, Japan*

(Received 18 March 2009; accepted 27 May 2009; published online 19 June 2009)

The authors report the buildup fabrication and magnetic domain characterizations of anisotropic-shaped MnAs nanoclusters position-controlled on partially SiO_2-masked GaAs (111)*B* substrates by selective-area metal-organic vapor phase epitaxy. Magnetic force microscopy reveals that both the symmetric- and anisotropic-shaped nanoclusters show spontaneous magnetization at room temperature. Some of the nanoclusters show a single magnetic domain, in which magnetized directions are along one of the *a*-axes of NiAs-type MnAs, after the external magnetic fields up to 3500 Gauss are applied in-plane. The magnetic domains are well controlled by introducing both magnetocrystalline and shape magnetic anisotropies in the anisotropic-shaped nanoclusters. © *2009 American Institute of Physics*. [DOI: 10.1063/1.3157275]

Recent research activities for heteroepitaxial nanostructures of ferromagnet and III-V compound semiconductor (FM III-V hybrids) have gained much attention in the future nanospintronic device applications.[1] It was reported that large tunneling magnetoresistance effect was shown in the MnAs/AlAs/MnAs heterostructures[2] and the GaAs:MnAs granular layers[3,4] above room temperature (RT), and that ferromagnetic NiAs-type MnAs layers served as an electrical spin injection source for semiconductors.[5] In recent theoretical calculations, in addition, it has been predicted that the electronic band-structure of hypothetical zinc-blende (ZB)-type MnAs layers is half-metallic, which is promising nature for device applications.[6–8] Thus far, conventional approaches to realizing nanospintronic devices using FM III-V hybrids have been mostly "top-down" fabrication techniques after the epitaxy because it has been necessary to grow the epitaxial ferromagnetic and semiconducting layers by molecular beam epitaxy at an extremely low growth temperature.[2–5,9] We have demonstrated the epitaxy of ferromagnetic NiAs-type MnAs nanoclusters (NCs) self-assembled on GaInAs/InP (111)*B* wafers by metal-organic vapor phase epitaxy (MOVPE).[10,11] For the NiAs-type (or ZB-type) MnAs growth, the {111} orientations of ZB-type layers are promising because of the similarity of their crystal structures. Another potential advantage in using the {111} orientations is the catalyst-free "buildup" fabrication of one-dimensional (1D) semiconductor nanowires (NWs) and ferromagnet/semiconductor heterostructured NCs position-controlled on semiconductor wafers by selective area MOVPE (SA-MOVPE) because atomically flat crystal facets and abrupt heterointerfaces are formed without any process-induced damage and contaminations. We have demonstrated the buildup fabrication of not only 1D NWs[12,13] but ferromagnetic NiAs-type MnAs NCs[14,15] on (111)*B* semiconductor wafers by SA-MOVPE. Our technique makes it possible to realize magnet tunnel junctions (MTJs) in a vertical and/or lateral geometry on semiconductor wafers. This is presumably favored because such device structures offer a large degree of freedom in their fabrication and possible integration on semiconductor devices. In addition, it has been predicted by theoretical calculations that magnetoresistance effects are tuned by tailoring MnAs NC arrangements on semiconductor wafers.[16] It is crucial for realizing MTJ-NCs in a vertical and/or lateral geometry to control coercive forces and magnetized directions, i.e., parallel and antiparallel states in each of the MnAs NCs designed to have a different shape and volume by tailoring the initial mask openings. In this letter, therefore, we report the buildup fabrication of anisotropic-shaped NiAs-type MnAs NC arrays, which possibly introduce both magnetocrystalline and shape magnetic anisotropies, on partially SiO_2-masked GaAs (111)*B* wafers by SA-MOVPE. This letter describes the experimental results of magnetic domain characterizations for the NCs.

We prepared GaAs (111)*B* substrates covered with periodic SiO_2 mask opening array patterns for the growth. The details of the substrate preparation for the symmetric-shaped MnAs NC growth were given elsewhere.[15] For the anisotropic-shaped MnAs NC growth, we fabricated two types of the initial mask patterns with the elongated mask openings in a triangular or square lattice arrangement within a 50×50 μm^2 area. The mask pattern of one type is the one that the major axes of the elongated mask openings are inclined by 90° (or 30°) from one of the *a*-axes of the NCs, or the minor axes are parallel to one of them, and that of the other type is the one that the major axes are parallel to one of the *a*-axes. Hereafter, these two patterns are referred to as "type-I" and "type-II," respectively. $(CH_3)_3Ga$, $(CH_3)_3Al$, $(CH_3C_5H_4)_2Mn$ and 20%-AsH_3 diluted in H_2 were used as source materials for SA-MOVPE.[17] The growth temperature, T_g, and the V/Mn ratio, whose definition was given elsewhere,[10] were 800–850 °C and 375–1125, respectively. MnAs NCs were formed directly on partially SiO_2-masked GaAs (111)*B* wafers (Figs. 1 and 2) or after the AlGaAs nanopillar growth on the wafers (Figs. 3 and 4). Size and

a)Author to whom correspondence should be addressed. Electronic mail: hara@rciqe.hokudai.ac.jp. Tel.: +81-11-706-7170. FAX: +81-11-716-6004.

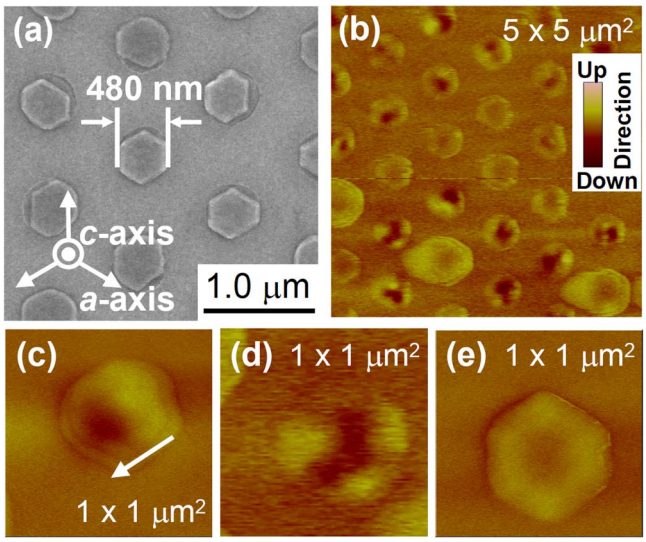

FIG. 1. (Color online) (a) SEM top view of the symmetric-shaped NCs. (b) MFM image of the as-grown NCs observed in (a). The as-grown NCs typically had three types of magnetic domains shown from (c) to (e).

crystal facets of the NCs were observed by scanning electron microscopy (SEM). We characterized magnetic domains of the NCs by magnetic force microscopy (MFM) at RT.

Initially, we investigated hexagonal symmetric-shaped NiAs-type MnAs NC array, whose period was 1 μm in a triangular lattice arrangement, position-controlled on the GaAs (111)*B* substrates with the SiO_2 mask opening size of 300 nm by SA-MOVPE. The T_g and V/Mn ratio were 850 °C and 375, respectively. Figure 1(a) shows a SEM top view of the NC array. Typical NCs measured 180 nm high and 480 nm wide. MFM for the "as-grown" NCs revealed

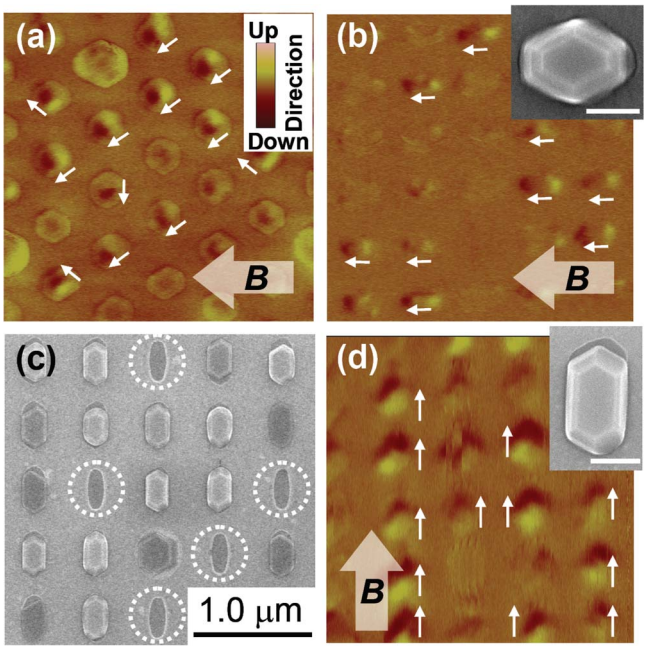

FIG. 2. (Color online) MFM images of (a) the symmetric-shaped and (b) the type-I NCs after applying ***B*** of 3500 Gauss in-plane. (c) SEM top view of the type-II NCs. No NC was grown in some of the initial mask openings marked by white-dotted circles. (d) MFM image of the NCs in (c) after applying ***B*** of 3500 Gauss in-plane. The insets in (b) and (d) show highly magnified SEM images for a typical NC, and white scale bars represent 300 nm. Scan area for MFM was 5.0×5.0 μm^2.

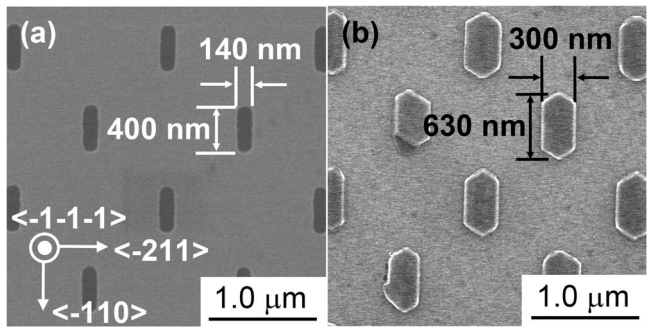

FIG. 3. SEM top views of (a) the initial SiO_2 mask openings on a GaAs (111)*B* substrate and (b) highly uniform type-II MnAs NCs on AlGaAs nanopillar buffers.

that magnetic responses were taken only for the MnAs NCs grown in the SiO_2 mask openings, and that no significant signal was detected for the SiO_2 masks covered on GaAs wafers, as shown in Figs. 1(b)–1(e). Some of the observed as-grown NCs seemed to have a single magnetic domain, which shows spontaneous magnetization, without any application of external magnetic fields. The observed NCs had typically three types of magnetic domains, as shown in Figs. 1(c)–1(e). Magnetic domains of one type shown in Fig. 1(c) clearly were a single magnetic domain whose magnetization direction was in-plane. Those of another type shown in Fig. 1(d) presumably were multimagnetic domains, and those of the other type shown in Fig. 1(e) possibly were closure mag-

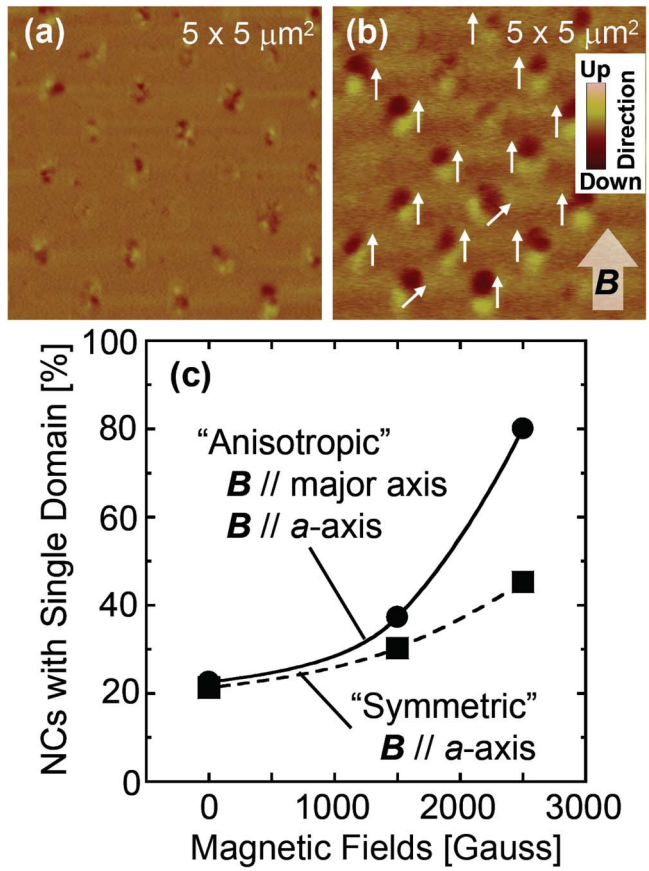

FIG. 4. (Color online) MFM images of (a) as-grown type-II NCs and (b) the NCs after applying ***B*** of 2500 Gauss in-plane. (c) Dependence of percentages of the NCs with a single magnetic domain in the observed MFM images on ***B***. For (c), the symmetric-shaped NCs typically measured 650 nm in diameter, and the anisotropic-shaped ones were shown in Fig. 3(b).

netic domains because it has been reported from both theoretical and experimental viewpoints that the vortex core with upward magnetizations, which is reflected by a dark and bright contrast in a MFM image, is supposed to be observed.[18] Figure 2(a) shows a MFM image of the symmetric-shaped MnAs NCs after the external magnetic fields, $\boldsymbol{B}$, of 3500 Gauss were applied in-plane. The magnetized directions, which were marked by white thin arrows in the MFM images and mainly originated from a magnetocrystalline anisotropy, in the NCs had a clear tendency to be along the applied magnetic fields direction. All the results above are consistent with the structural characterization results, in which *a*-axes, magnetic easy axes, of the symmetric-shaped MnAs NCa are in-plane, obtained by cross-sectional transmission electron microscopy (TEM).[15] However, it is still difficult to control thoroughly the magnetized directions of all the NCs because of three equivalent magnetic easy axes, *a*-axes, of MnAs. Subsequently, therefore, we fabricated anisotropic-shaped MnAs NCs to introduce both magnetocrystalline and shape magnetic anisotropies. In order to closely characterize magnetic domains in the anisotropic-shaped NCs, we investigated two types of the anisotropic-shaped NCs using type-I and type-II patterns. The aspect ratio of the initial mask openings was about 2.4 for both patterns. Typical type-I NCs measured about 600 nm along the major axis and 540 nm along the minor one, and their aspect ratio was 1.3. Typical type-II ones, on the other hand, measured about 675 and 375 nm, respectively, and their aspect ratio was 1.8. The difference in the aspect ratios of the type-I and type-II NCs was caused by the relationship between the *a*-axis of the NCs and the major axis of the initial mask openings. Figure 2(b) shows a MFM image of the type-I NCs. When $\boldsymbol{B}$ of 3500 Gauss were applied along the major axis direction of the NCs ($\boldsymbol{B}\parallel$ major axis), which was perpendicular to one of the *a*-axes of the type-I NCs ($\boldsymbol{B}\perp$ *a*-axis), it was observed that some of the NCs had a single magnetic domain, which was possibly originated from a shape magnetic anisotropy. Figure 2(c) shows a typical SEM image of the type-II NCs. Hexagonal anisotropic-shaped MnAs NC array was formed in a square lattice arrangement, whereas we observed that no MnAs NC was formed in some of the initial mask openings, as in the case marked by white dotted circles. These missing NCs were similarly observed for the type-I NCs (not shown here). Figure 2(d) shows a MFM image of the NCs observed in Fig. 2(c) after applying $\boldsymbol{B}$ of 3500 Gauss parallel to both the major axis direction and one of the *a*-axes of the NCs ($\boldsymbol{B}\parallel$ major- and *a*-axes). The type-II NCs showed much stronger magnetic response of a single magnetic domain, which was presumably because the magnetization was preferably along the *a*-axis parallel to the major axis direction, as shown in Fig. 2(d). In the other two cases, i.e., $\boldsymbol{B}\perp$ major axis and $\boldsymbol{B}\parallel$ *a*-axis for the type-I NCs and $\boldsymbol{B}\perp$ major- and *a*-axes for the type-II NCs, almost no controllability in the magnetized directions of the NCs was observed (not shown here). In the case of the samples shown in Figs. 1(a) and 2(c), the size uniformity of the NCs was not so high because of the unintentional deposition of GaAs layers under the MnAs NCs, which was investigated by TEM in our previous work.[15] Finally, therefore, we report the formation and magnetic characterizations for the anisotropic-shaped MnAs NCs with a high degree of uniformity. On a template substrate shown in the SEM image of Fig. 3(a), the type-II NCs were formed after the MnAs growth on AlGaAs nanopillar buffers, as shown in Fig. 3(b). Typical NCs measured about 630 nm along the major axis and 300 nm along the minor one, and their aspect ratio was 2.1. Highly uniform anisotropic-shaped MnAs/AlGaAs NCs were formed in all the initial mask openings, in contrast with the case shown in Fig. 2(c), in which some of the MnAs NCs were missing. Figures 4(a) and 4(b) show MFM images of as-grown type-II MnAs/AlGaAs NCs and of the NCs after applying $\boldsymbol{B}$ of 2500 Gauss parallel to both the major axis direction and one of the *a*-axes of the NCs ($\boldsymbol{B}\parallel$ major- and *a*-axes), respectively. We observed a clear magnetic response indicating that most of the NCs had a single magnetic domain, as shown in Fig. 4(b), while almost all the as-grown NCs in Fig. 4(a) seemed to have a multimagnetic domain. Figure 4(c) shows the detailed dependences of the percentages of the NCs with a single magnetic domain in the observed MFM images for both the symmetric-shaped and the type-II MnAs/AlGaAs NCs on $\boldsymbol{B}$. The percentage of the type-II NCs with a single magnetic domain increased up to about 80% with increasing $\boldsymbol{B}$ to 2500 Gauss, whereas that of the symmetric-shaped NCs was as high as 43%. Therefore, we concluded that magnetic domains and the magnetized directions of the type-II NCs were well controlled presumably owing to the introduction of both magnetocrystalline and shape magnetic anisotropies into the NCs. We believe that our technique is promising for realizing MTJ-NCs in a vertical and/or lateral geometry by tailoring the initial mask openings to tune coercive forces and magnetized directions in each of the NCs.

The authors thank J. Motohisa, K. Hiruma, T. Sato, H. Yoshida, and A. Hayashida for fruitful discussions. This work was supported by JST-PRESTO and a Grant-in-Aid for Scientific Research from the MEXT of Japan.

[1]M. Tanaka, J. Cryst. Growth **278**, 25 (2005).
[2]V. Garcia, H. Jaffres, M. Eddrief, M. Marangolo, V. H. Etgens, and J.-M. George, Phys. Rev. B **72**, 081303 (2005).
[3]M. Yokoyama, T. Ogawa, A. M. Nazmul, and M. Tanaka, J. Appl. Phys. **99**, 08D502 (2006).
[4]P. N. Hai, K. Takahashi, M. Yokoyama, S. Ohya, and M. Tanaka, J. Magn. Magn. Mater. **310**, 1932 (2007).
[5]M. Ramsteiner, H. Y. Hao, A. Kawaharazuka, H. J. Zhu, M. Kästner, R. Hey, L. Däweritz, H. T. Grahn, and K. H. Ploog, Phys. Rev. B **66**, 081304 (2002).
[6]M. Shirai, T. Ogawa, I. Kitagawa, and N. Suzuki, J. Magn. Magn. Mater. **177–181**, 1383 (1998).
[7]S. Sanvito and N. A. Hill, Phys. Rev. B **62**, 15553 (2000).
[8]Y.-J. Zhao, W. T. Geng, A. J. Freeman, and B. Delley, Phys. Rev. B **65**, 113202 (2002).
[9]D. Saha, M. Holub, P. Bhattacharya, and Y. C. Liao, Appl. Phys. Lett. **89**, 142504 (2006).
[10]S. Hara and T. Fukui, Appl. Phys. Lett. **89**, 113111 (2006).
[11]S. Hara, J. Motohisa, and T. Fukui, J. Cryst. Growth **298**, 612 (2007).
[12]J. Motohisa, J. Noborisaka, J. Takeda, M. Inari, and T. Fukui, J. Cryst. Growth **272**, 180 (2004).
[13]J. Noborisaka, J. Motohisa, S. Hara, and T. Fukui, Appl. Phys. Lett. **87**, 093109 (2005).
[14]S. Hara, D. Kawamura, H. Iguchi, J. Motohisa, and T. Fukui, J. Cryst. Growth **310**, 2390 (2008).
[15]T. Wakatsuki, S. Hara, S. Ito, D. Kawamura, and T. Fukui, Jpn. J. Appl. Phys. **48**, 04C137 (2009).
[16]C. Michel, M. T. Elm, B. Goldlücke, S. D. Baranovskii, P. Thomas, W. Heimbrodt, and P. J. Klar, Appl. Phys. Lett. **92**, 223119 (2008).
[17]S. Hara and A. Kuramata, Nanotechnology **16**, 957 (2005).
[18]T. Shinjo, T. Okuno, R. Hassdorf, K. Shigeto, and T. Ono, Science **289**, 930 (2000).